

Spatio and Efficient ℓ_1 - ℓ_1 minimization based Impulse Noise Removal in Gray Images Using Dictionary Learning

P.Jothibas, *Member, IAENG*, and P.Rangarajan

Abstract—In natural images spatially adjacent image pixels have similar pixel values and many patches of image pixels have similar values. This similarity exploited for reducing the computation time required for de-noising and ℓ_1 - ℓ_1 minimization was modified for efficient implementation. Using impulse noise detector, noisy pixels were separated and from noise free pixels DC values of image batches were calculated. This accurate DC value calculation improves the quality of the de-noised image and preserves the details. Once noise is removed using efficient ℓ_1 - ℓ_1 minimization, de-noised pixels will replace noisy pixel in the corrupted image. The proposed algorithm gives superior peak signal-to-noise ratio (PSNR) and structural similarity (SSIM) indices compared with the other state-of-the-art algorithms for grey images.

Index Terms—Augmented Lagrangian Multiplier, Dictionary Learning, Impulse noise removal, Sparse Representation

I. INTRODUCTION

OUR brains are able to recognize a human face and other shapes and details in a fraction of time by comparing it with the stored image in the neurons. The brain can recognize images corrupted to the certain extent. Brain can conjure the details behind the corrupted images, but our image processing algorithms fail to extract certain details from the image, when the image is corrupted by different types of noises and other artifacts. Image details are required for image registration, segmentation, comparison, recognition of objects and retrieval. Image corruption may occur at any stage of image acquisition process. Image acquisition process consists of three stages, viz., acquisition, transmission, and storage. Image acquisition is affected by the image sensor, environment of the imaging subject, and imaging expert. In controlled environment image corruption is less due to environment. In uncontrolled environment like underwater, extreme temperatures, hazardous situations, inaccessible remote areas, and uncontrolled light conditions, image corruption is unavoidable during acquisition. It requires a further processing of an image being essential to improve the quality and to extract the details. Corruption may be blurring, Gaussian noise, defocus etc. During the transmission of the acquired image from the imaging device to other places for dissemination, it may get corrupted. Transmission may be done using wired or wireless channel or memory. Imperfections in the channel and disturbances by

adjacent devices or equipments may corrupt the image. Third type of image corruption occurs during storage of images in the memory. System constrained and limitation of the memory size leads to restricted number of images stored per memory device. Programming error and large number of functionalities in user computer may lead to image corruption in memory. Latest developments and technological breakthrough are able to address certain issues in image acquisition process to obtain noise free images. Still certain cases of image corruption are unavoidable. This necessitates the use of computationally efficient and qualitatively better de-noising algorithms. With this objective many algorithms have been designed. Image de-noising algorithms may be linear or non-linear based upon the relationship between the input and the output. Linear algorithms [1], [2] are mean and its variants. Mean is used to remove the additive Gaussian noises and multiplicative noise. Mean filters fail to de-noise the high density noises and leave smoothing effect on the final image output [1], [2]. Non-linear filters such as median filters are more appropriate for removing salt and pepper impulse noise in the image, perform better to remove the outliers [1], [2]. Wavelet based de-noising is also proposed for Gaussian corrupted images and speckle noise corrupted images. Different types of shrinkages such as the soft shrinkage, hard shrinkage, Bayes shrink, Bishrink are used to remove the noise in wavelet domain. Wavelet based de-noising methods are not capable of producing an appreciable de-noising performance for high density impulse noises.

Recently Sparse representation and over-complete dictionary have received much attention [13], [15]–[17]. Sparse representation has been used in different post image processing applications such as super resolution [21], facial expression recognition [25], compression [23], face recognition [22], text detection [26], Spectral Estimation [19], Pedestrian detection [27] and also in de-noising [24]. There are many sparse representation based de-noising methods such as K-SVD [30], Sparse representation using Augmented Lagrangian Multiplier based de-noising [10], ℓ_1 - ℓ_1 [9], AK-SPR [8], ℓ_1 -TV [7] and numerous other algorithms exist for additive Gaussian de-noising, but very few research articles on salt and pepper impulse noise, de-noising have been published. In this paper Spatial and efficient ℓ_1 - ℓ_1 minimization (SELL) based image de-nosing method is attempted.

The outline of the paper is as follows: In Section II, we review some of the related works. In Section III, we propose a block diagram and algorithms for removal of fixed value impulse noise and random value impulse noise. In Section IV, numerical experiments of the proposed algorithm and

Manuscript received September 10, 2014; revised April 18, 2015.

P.Jothibas, Asst. Professor is with the Department of Electronics and Instrumentation Engineering, R.M.K. Engineering College, Chennai-601206, India and also a Research Scholar, Anna University, Chennai-600025, India e-mail: (jothibasuin@gmail.com).

R.Rangarajan, Professor, Department of Electrical and Electronics Engineering, R.M.D. Engineering College, Chennai-601206, India.

its results are discussed to demonstrate the performance improvement by the proposed algorithm. In Section V, discussions on parameter settings, DC value calculations and computational calculations are presented. Section VI concludes the paper with findings and a statement on future direction.

II. DERIVATION OF ℓ_1 - ℓ_1 MINIMIZATION

Sparse representation based salt and pepper impulse noise removal and random valued noise removal presented in references [9]–[12] are reviewed in this section. This section explains optimization using Augmented Lagrangian Multiplier based ℓ_1 - ℓ_1 -minimization and modification of algorithm for efficient implementation. Subsection II-A presents de-noising model for the image restoration. Subsection II-B explains modification of ℓ_1 - ℓ_1 minimization for efficient implementation. Subsection II-C explains the similar image batch identification, grouping, and generation of representative image batches for de-noising using efficient ℓ_1 - ℓ_1 minimization algorithm.

A. De-noising model

Let Im be the noise corrupted image of size $W \times W$ and ρ be the probability of noise intensity. Then corrupted image is represented in equation 1.

$$Im(s) = \begin{cases} Im_d(s), & \varepsilon \leq \rho \\ Im_0(s), & \varepsilon > \rho \end{cases} \quad (1)$$

where s denotes two dimensional indices of image Im , $Im_0(s)$ denotes noise free pixels in the image, $Im_d(s)$ stands for noise corrupted image pixels, s varies from 1 to W and ε -is a random number with range of values $[0,1]$. For Salt and Pepper Noise, $Im_d(s)$ takes either Im_{min} or Im_{max} . For Random value noise, $Im_d(s)$ takes any value in the range $[Im_{min}, Im_{max}]$, which is independently and identically distributed. \widehat{Im} - recovered de-noised image from corrupted image. Noisy image dimensions were $W \times W$. From noisy image, image batches were extracted by overlapping batches of size $\sqrt{M} \times \sqrt{M}$. Total number of batches from $W \times W$ image is $L = (W - \sqrt{M} + 1)^2$. M is the number of rows in the dictionary (A) and N is the number of columns in the dictionary (A). M and N value determination is explained in subsection V-A of section V. Each batch size, $\sqrt{M} \times \sqrt{M}$ is reshaped into column vector $b_i = [Im(s_{i1}), Im(s_{i2}), \dots, Im(s_{iM})] \in R^M$. These batches are represented as B .

$$B = [b_1, b_2, \dots, b_i, \dots, b_L] \in R^{M \times L}.$$

$$b_i = A_i X_i, i = 1, 2, 3, \dots, L,$$

b_i is represented by over complete dictionary A ,

where $A = [a_1, a_2, \dots, a_W] \in R^{M \times W}$ and X is a sparse coefficient.

$$\min_{A, X} \|X\|_0 + \alpha \|B - AX\|_2 \quad (2)$$

Where $X = [X_1, X_2, \dots, X_L] \in R^{W \times L}$ is the sparse coefficient. In equation 2 first term represents the sparse representation of X , which counts the few non-zero coefficient in the X , i.e sparse solution for X . $\|X\|_0$ is computationally intensive and $\|B - AX\|_2$ represents root mean square error between B and AX . Each column in A is called atom or basis, which represented as $a_j \in R^M$ atom or basis, each atom is

normalized as $\|a_j\|_2 = 1$. RMSE is susceptible to outliers such as salt and pepper impulse noise, so it is modified as ℓ_1 norm equation 3, to be robust enough for outliers.

$$\min_{A, X} \|X\|_0 + \alpha \|B - AX\|_1 \quad (3)$$

Based on learned dictionary values \widehat{A} and sparse coefficients \widehat{X} , de-noised image batches \widehat{b} are constructed as in equation 4.

$$\widehat{b} = \widehat{A}\widehat{X} \quad (4)$$

From batches \widehat{b} , image is reconstructed by averaging different estimates of same pixel.

B. Modification of ℓ_1 - ℓ_1 Minimization algorithmic equations

Equation for de-noising algorithms presented in [10], [11], [28] contains redundant similar terms and non-adaptive terms, which are reasons for high computational time and inaccurate results. Algorithmic equations were modified by deriving the new equation for Y , X and modifying the iterative shrinkage algorithms. Equation for X is given as

$$X^k = SHRINK(X^{k-1} + \frac{A^{k-1}Y^k}{\gamma U^{k-1}}, \frac{1}{\gamma U^{k-1}}) \quad (5)$$

$$\gamma = \max(\text{eig}(A^{kT}A)) \quad (6)$$

To simplify equation for Augmented Lagrangian Multiplier Y , assume U and τ as in equation 7 and 8.

$$U = -A^{k-1}X^{k-1} + b + \frac{Y^{k-1}}{\mu^{k-1}} \quad (7)$$

$$\tau = \frac{\alpha}{\mu^{k-1}} \quad (8)$$

Equation for Y is rewritten as

$$PROJ(U, \tau) = U - SHRINK(U, \tau) \quad (9)$$

$$SHRINK(U, \tau) = \begin{cases} U - \tau, & U > \tau \\ 0, & \tau \geq U \geq -\tau \\ U + \tau, & U < -\tau \end{cases} \quad (10)$$

Equation 9 and equation for Y is written as in equation 11

$$Y = \mu PROJ(U, \tau) = \mu U - \mu SHRINK(U, \tau) \quad (11)$$

Equation 10 is substituted in 9, to yield $PROJ(U, \tau) = \mu^{k-1}U - \tau^{k-1}SHRINK(U, \tau)$

$$= \mu^{k-1}U - \begin{cases} \mu^{k-1}U - \mu^{k-1}\tau, & U > \tau \\ 0, & \tau \geq U \geq -\tau \\ \mu^{k-1}U + \mu^{k-1}\tau, & U < -\tau \end{cases} \quad (12)$$

Again rearranging equation 12 we obtain 13. Constraints for 13 are not changed. We reduce the large amount calculation required to calculate the Y and also the overhead required for finding Y from using $PROJ$ and $SHRINK$. For large amount of image batches and number of iterations, it is essential to have optimized equations and algorithms. The straight forward equation for Y is given in equation 13

$$Y = \begin{cases} \mu^{k-1}\tau, & U > \tau \\ \mu^{k-1}U, & \tau \geq U \geq -\tau \\ -\mu^{k-1}\tau, & U < -\tau \end{cases} \quad (13)$$

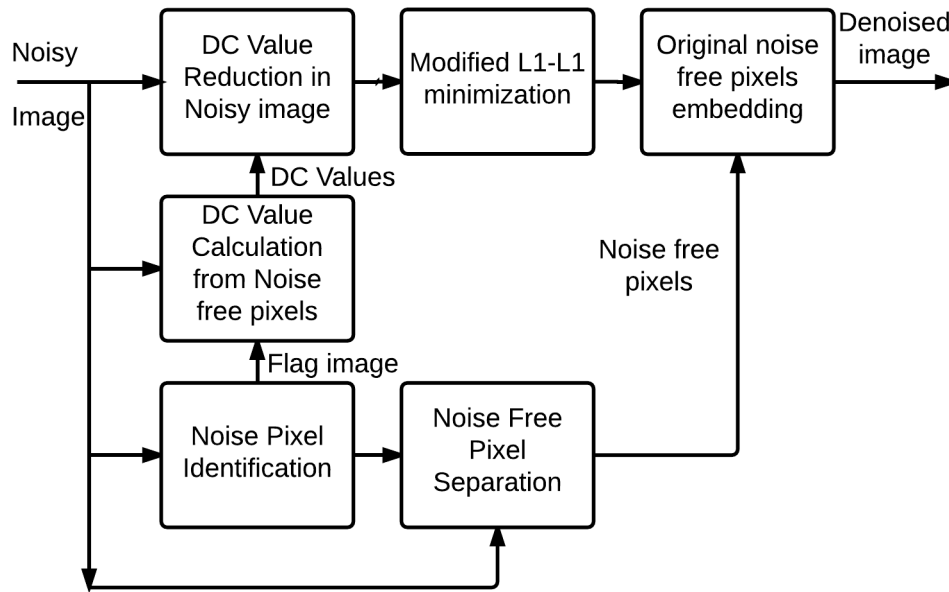


Fig. 1. Block diagram for the proposed denoising method for salt and pepper and random value impulse noises

$\tau = \frac{\alpha}{\mu^{k-1}}$, Substituting the value τ in the equation 13, we obtain 14

$$Y = \begin{cases} \alpha, & U > \tau \\ \mu^{k-1}U, & \tau \geq U \geq \tau \\ -\alpha, & U < \tau \end{cases} \quad (14)$$

$$A^k = A^{k-1} + \beta Y^k (X^{kT}) \quad (15)$$

C. Grouping by similarity

In natural images, there are many similar pixel batches, in which pixels have similar values. These batches may be located adjacent to each other or located some distances apart depending on image content. This notion of similarity is used to identify pixel batches and group them together. This similarity identification is carried out by finding the difference between batches. If the difference is below the threshold value T , then batches are considered similar. If the difference is greater than the threshold T , then batches are considered as dissimilar. And dissimilar batches are considered as a separate group of image batches. The relation for finding similar batches is given by in equation 16

$$b_i - b_j < T, \quad i \neq j \quad (16)$$

For similarity detection, at least 50% of pixels in the batches are to be noise free pixels. From each group, one batch of pixel is taken for denoising. Image batches are compared within the range of 10×10 window. This restriction on comparison reduces the computation complexity. When noise level increases, number of groups increases due to dissimilarity between noise free pixel batches.

III. BLOCK DIAGRAM AND ALGORITHMS

The block diagram of the proposed de-noising method and algorithms are explained in this section of the paper. Subsection III-A explains different stages of this noise removal

method. Subsection III-B explains the algorithms for DC value calculation and subsection III-C explains reconstruction of de-noised image.

A. Block diagram

Input for this method is corrupted image and output is de-noised image. Each pixel and its surrounding pixels of batch size $\sqrt{M} \times \sqrt{M}$ are considered for de-noising. Overlapping of pixels is essential in order to avoid the blocking artifacts in the resulting image. DC value calculation in the salt and pepper impulse noise corrupted image is difficult, because of extreme values of corrupted pixels in the image. Corrupted image pixels completely changed from their original value. Accurate DC value calculation is essential for the better de-noising by SELL. DC value calculation is done by combination of impulse noise detector and aggregation of median from noise free pixels. Calculated DC values are subtracted from raw image batches. Block diagram in Fig.1 contains blocks for Noise pixel identification, DC Value calculation and DC value reduction in noisy image. Subtracted DC values are added to the de-noised image after modifying $\ell_1 - \ell_1$ minimization based de-noising.

Noise pixels are identified using any impulse and random value noise detector method [18]. Modified $\ell_1 - \ell_1$ minimization block uses Augmented Lagrangian Multiplier based minimization method for impulse noise removal algorithm. Its derivation is given in the subsections II-A and II-B of section II. Detailed algorithm with modification to reduce the computation time is given in section II-C. In the noise pixel replacement block, noisy pixels of corrupted image are replaced by corresponding de-noised pixels from modified $\ell_1 - \ell_1$ minimization. The algorithm 3 in section III-C explains the embedding of original noise free pixel in de-noised image.

B. DC value calculation from noise free pixels

DC values are calculated accurately after detecting the noisy pixel in the image batches based on any impulse noise detection algorithm. From impulse detection binary flag image f is generated. And binary image f is inverted and multiplied by noisy image Im to obtain the noise free pixels in the image as in equation 17. Median of noise free pixels is considered as a DC value for each image batch, which will be subtracted from the image batches before applying the de-noising algorithm.

C. Final De-noised image

Binary flag image f , corrupted image Im and de-noised image \widehat{Im} from algorithm 1 are used to reconstruct the final de-noised image as in equation 17.

Algorithm 1 DC value calculation from the noise free pixels of noisy image patches.

f - Binary flag image (1- noisy pixel, 0- noise free pixel)

Im - Noisy image

- 1: Noise Free pixels in a image = $(\sim f) Im$
 - 2: Segregated noise free pixels and zero value pixels are converted into batches of 8×8 pixels and each batch is converted into column matrix.
 - 3: Calculate Median of each column matrices.
-

Algorithm 2 Modified $\ell_1 - \ell_1$ Minimization using Augmented Lagrangian Multiplier

$\gamma^0 = \max(\text{eig}(A^0 T A^0))$ - Initial value

b - DC values of subtracted image batches

Initialize $X_0 = 0, Y_0 = 0, \mu_0 = 0.006$

A^0 = DCT Dictionary or random values

WHILE(Stopping criterion is not satisfied, continue looping)

- 1: $U = -A^{k-1} X^{k-1} + b + \frac{Y^{k-1}}{\mu^{k-1}}, \tau = \frac{\alpha}{\mu^{k-1}}$
- 2:

$$Y^k = \begin{cases} \alpha, & U > \tau \\ \mu^{k-1} U, & \tau \geq U \geq \tau \\ -\alpha, & U < \tau \end{cases}$$

- 3: $X^k = \text{SHRINK}(X^{k-1} + \frac{A^{k-1} Y^k}{\gamma U^{k-1}}, \frac{1}{\gamma U^{k-1}})$
- 4: $A^k = A^{k-1} + \beta Y^k (X^k)^T$
- 5: $A^k = A^k \cdot \text{diag}(\|a_0^k\|_2^{-1}, \|a_1^k\|_2^{-1}, \dots, \|a_N^k\|_2^{-1})$
- 6: $\gamma = \max(\text{eig}(A^{k T} A^k))$
- 7: $\mu^k = 1.01 \mu^{k-1}$

ENDWHILE

Algorithm 3 Final Image construction

f - Binary flag image (1- noisy pixel, 0- noise free pixel)

Im - Noisy image

\widehat{Im} - De-noised pixels of noisy image by efficient $\ell_1 - \ell_1$ minimization for which binary Flag image value is 1

$$\text{Final Image} = (\sim f) Im + (f) \widehat{Im} \quad (17)$$

IV. EXPERIMENTS AND RESULTS

Experiments were conducted on many standard images. Images used to demonstrate the performance of the proposed algorithm were girl, boat, baboon, Barbara, house, airplane, lake, bridge, peppers, Lena, parrot, cameraman etc. Most of the images used for testing were of size 256×256 , if size of the image is 512×512 , which were converted to 256×256 image by considering the alternate pixels in the image.

The proposed algorithm was compared with many spatial and sparse representation based algorithms. Spatial domain algorithms implemented for comparison were PSMF [4], ACWM [5], DWM [6] and Sparse representation based algorithms were L1-TV [7], AK-SPR [8]. Image metrics used for comparison of algorithms performance were peak-signal to noise ratio (PSNR), mean square error (MSE), and structural similarity index (SSIM) [20]. The equation for metrics are given in 18, 19, and 20.

$$\text{PSNR} = 10 \log_{10} \frac{(2^b - 1)^2}{\text{MSE}} \quad (18)$$

$$\text{MSE} = \frac{\sum_{m=0}^{N-1} \left(\sum_{n=0}^{M-1} (Im(m, n) - Im_0(m, n))^2 \right)}{N^2} \quad (19)$$

$$\text{SSIM} = \frac{(2\mu_0\mu_{I_0} + C_1)(2\sigma_{I_0,0} + C_2)}{(\mu_0^2 + \mu_{I_0}^2 + C_1)(\sigma_0^2 + \sigma_{I_0}^2 + C_2)} \quad (20)$$

μ_0 - Mean intensities of original image, μ_{I_0} - Mean Intensities of restored image, $\sigma_{I_0,0}^2$ - Co-variance of original and restored image, σ_0 - Standard deviation of the original image, σ_{I_0} - Standard deviation of the restored image image.

Dictionary size for the experiments was 64×256 . Size of each basis or atom was 64 and the number of atoms was 256. The size of the dictionary was fixed after experimenting various values for better PSNR value. The details of experiments are given in subsection A of section V. Dictionary size was fixed at 64×256 . After experiments μ value was fixed at 0.006. μ value was updated after each iteration. Number of iterations for the loop was fixed at 25. And value for $\beta = 0.001$. DC values of the image batches were calculated after excluding noisy pixel values in the image batches and DC values were subtracted from the image batches before applying SELL based de-noising algorithm to the image batches. DC values were calculated based on the median of the noise free pixels, instead of mean. Mean is suitable for DC value calculation of Gaussian noise corrupted images. In salt and pepper impulse noise and random value impulse noise median is best suited for DC value calculation because of extreme values of noisy pixels. $\gamma = \max(\text{eig}(A^T A))$ was calculated adaptively after updating and normalizing the dictionary A.

Two types of initial dictionary values were used in experiments. One is based on DCT as initial value for dictionary and another is random values as a initial value for dictionary. The final dictionary values did not change after 40 iterations, regardless of initial dictionary values. The proposed algorithm is robust to the initial dictionary values. If random matrix is considered as an initial dictionary, γ value varies from larger value to smaller value during different iterations of SELL algorithm. After 20 iterations γ value confines itself to small range of values. In case of DCT matrix as

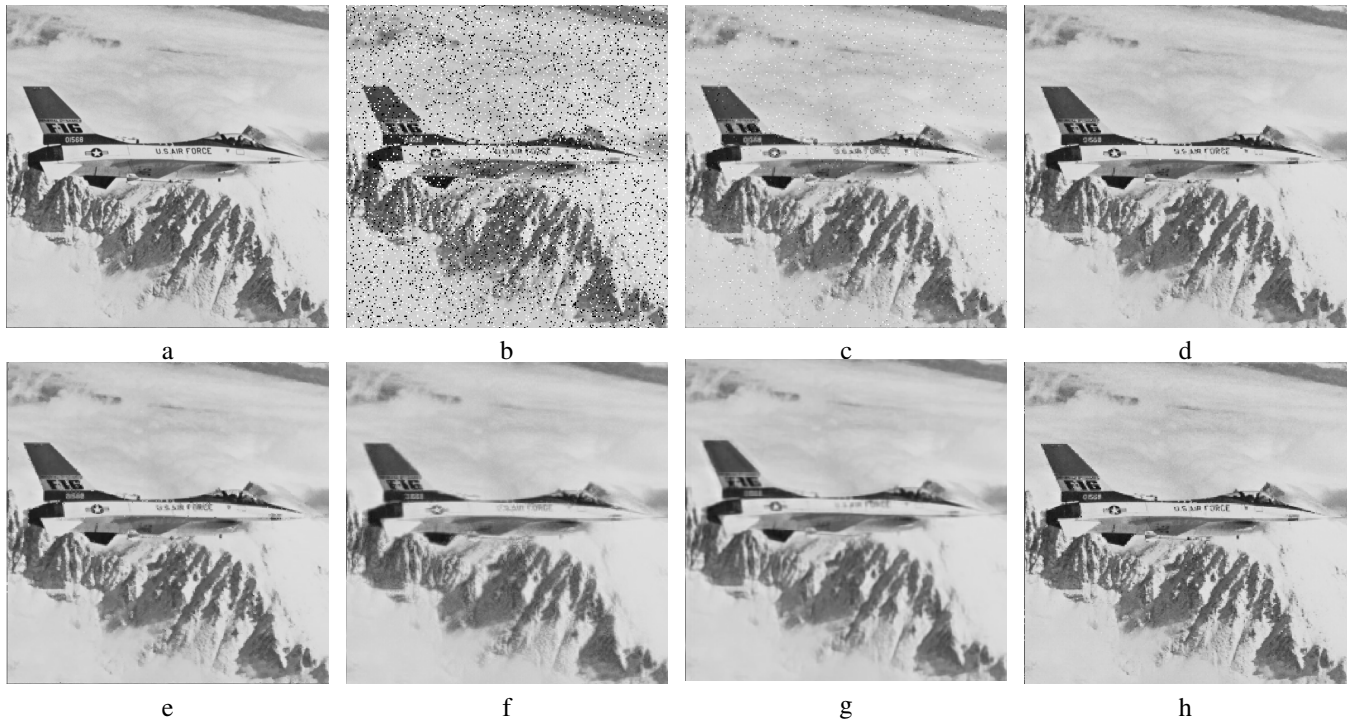


Fig. 2. The denoising results for airplane image corrupted by fixed value impulse noise a) original airplane image b) 10% of pixels corrupted by salt and pepper impulse noise c) PSMF d) ACWM e) DWM f) $l1l1$ -DCT g) DL-INR h) The proposed method

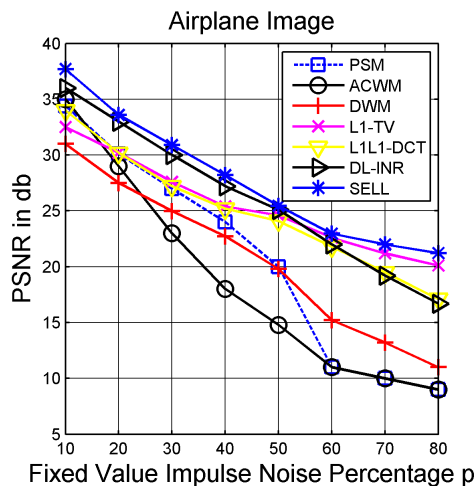


Fig. 3. PSNR values for various percentage of fixed value impulse noise corrupted pixels in airplane image

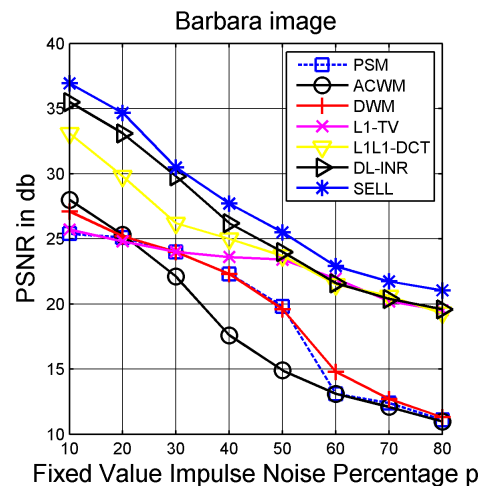


Fig. 4. PSNR values for various percentage of fixed value impulse noise corrupted pixels in barbara image

an initial dictionary matrix, γ value increases from smaller value to larger value and stabilizes to constant value. In the experiments, noise density varied from 10% to 80%. After 90% salt and pepper noise and random value noise, dictionary updation fails due to very large Eigen values. Further refinement of algorithm is required for very high density noisy image, which will be carried out in our future work.

A. Fixed value impulse noise removal

In fixed value or salt and pepper impulse noise removal experiments, images were corrupted by impulse noise in the range of 10% to 80%. Six standard images were used for the experiments. Fig.2,5,6 shows the result of proposed algorithm and five other algorithms for 10%-30% noise corrupted images.

Fig.2(a) is original airplane image. Fig.2 (b) is 10% noise corrupted image. Fig.2 (c), (d), (e), (f), (g) and (h) are the de-noising results of PSMF, ACWM, DWM, $l1l1$ -DCT, DL-INR and the proposed algorithms. Among the de-noising algorithm results, PSMF, ACWM, DWM, $l1l1$ -DCT, DL-INR algorithms are able to recover an image with edge and detail preservation. PSMF algorithm leaves few batches in the de-noised image. In $l1l1$ -DCT algorithm smoothens the image. $l1l1$ -DCT does not update its dictionary and its de-noising result is blurred. SELL algorithm's de-noising results has clarity and contrast of the image is comparable to that of original and better than DL-INR algorithm. The letters on the airplane image is visible and better than other algorithms. Other algorithms results are poor for higher noise densities. PSNR values of spatial domain filters are less than the sparse domain filters and the proposed algorithm has higher PSNR



Fig. 5. The denoising results for barbara image corrupted by fixed value impulse noise a) original barbara image b) 20% of pixels corrupted by salt and pepper impulse noise c) PSMF d) ACWM e) DWM f) $\ell 1\ell 1$ -DCT g) DL-INR h) The proposed method

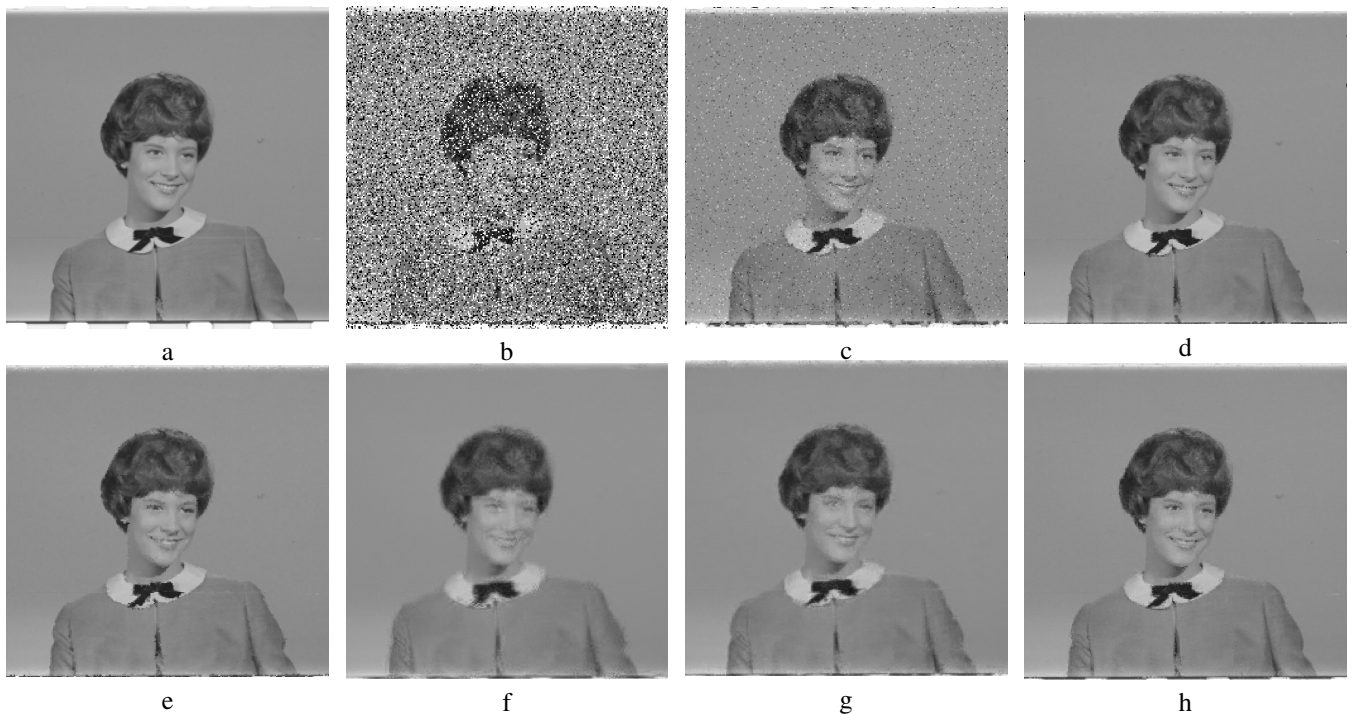


Fig. 6. The denoising results for girl image corrupted by fixed value impulse noise a) original girl image b) 30% of pixels corrupted by salt and pepper impulse noise c) PSMF d) ACWM e) DWM f) $\ell 1\ell 1$ -DCT g) DL-INR h) The proposed method

value than the other sparse domain algorithms as shown in Fig.3.

Fig.5 (a) shows standard barbara image, Fig.5 (b) shows 20% of pixels corrupted in barbara image. Fig.5 (c), (d), (e), (f), (g) and (h) shows the denoising results of the proposed algorithm and other algorithms. Fig.5 (h) shows that the proposed algorithm able to recover details of background, scarf and cloth than other algorithms. PSNR values of the DL-INR and $\ell 1\ell 1$ -DCT are slightly less than the proposed algorithm PSNR values as shown in Fig.4.

Fig.6 shows the denoising results of algorithms, original image and corrupted image of girl standard image. The denoising results of the proposed algorithm is better than other algorithms. The proposed algorithm recovers the details like eyes, tie and hair of the girl image better than all algorithms. Fig.6 (c) is the denoising result of PSMF algorithm, which contains few unfiltered pixels. Results of DL-INR and $\ell 1\ell 1$ -DCT contains blurred eyes and other details. ACWMF and DWMF algorithm outputs are comparable with the proposed algorithm output. For higher density noises these

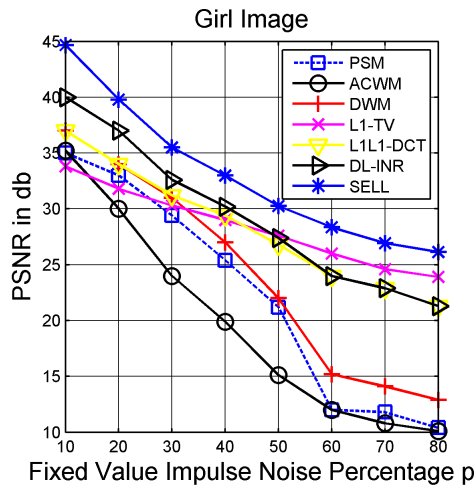


Fig. 7. PSNR values for various percentage of fixed value impulse noise corrupted pixels in girl image

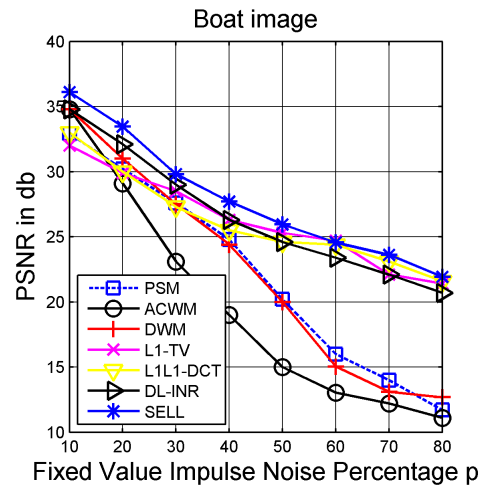


Fig. 9. PSNR values for various percentage of fixed value impulse noise corrupted pixels in boat image

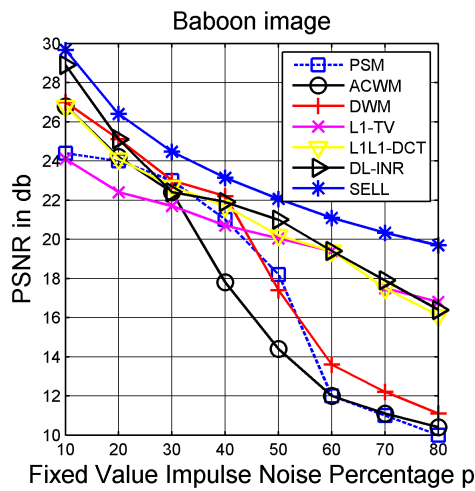


Fig. 8. PSNR values for various percentage of fixed value impulse noise corrupted pixels in baboon image

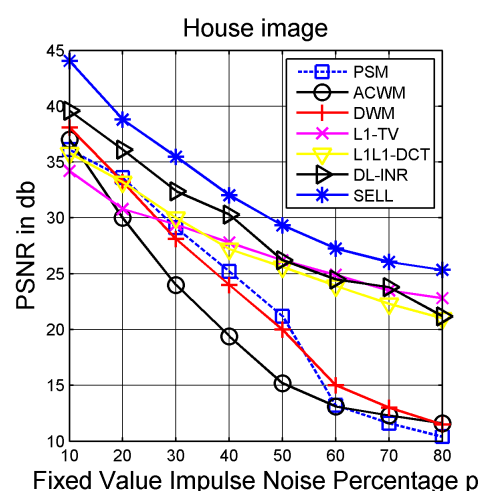


Fig. 10. PSNR values for various percentage of fixed value impulse noise corrupted pixels in house image

two algorithms produces degraded images. PSNR values of the ACWMMF and DWMF are less than the proposed algorithm PSNR values as shown in Fig.7.

Fig.3,4,7,8,9,10 shows the plots between PSNR and fixed value impulse noise density for standard images. In each plot proposed algorithm is compared with many standard algorithms. The proposed algorithm outperforms all other state-of-the-art algorithms in terms of peak signal to noise ratio (PSNR) and structural similarity index(SSIM). From Fig.3,4,7,8,9,10, it is understood that PSNR of SELL algorithm is appreciably higher than the other algorithms.

SSIM results shown in Table I compare the DL-INR algorithm with SELL algorithm. SELL algorithm performs better in terms of structural restoration of images corrupted by the salt and pepper impulse noise. SSIM values are calculated from the average of 10 experiments for each image.

B. Random value impulse noise removal

Random value impulse noise was applied to standard test images and the performance of the different de-noising algorithms were obtained for comparison. Noise density varied from 10% to 80% and the corresponding PSNR and

SSIM values were calculated and tabulated. Fig.11,14,17 shows denoising results of various algorithms for various standard images and different noise levels.

Fig.11 shows the denoising results of 50% of pixels in boat image corrupted by the random value impulse noise. Denoising results of various algorithms were shown in figure Fig.11 (c), (d), (e), (f), (g) and (h). When 50% of pixels are corrupted by random value impulse noise, most of the spatial domain algorithms gives a blurred image. The details like poles at the top of the boat, stones at the bottom of the boat and letters on the back of the boat were blurred beyond recognition in other algorithm results than the proposed algorithm. PSNR values were plotted against percentage of pixels corrupted by the random values impulse noise shown in Fig.13 and PSNR values also higher for the proposed algorithm than other algorithms.

Fig.14 shows the original test image baboon, 70% of pixels corrupted by random value impulse noise and denoising results of standard de-noising algorithms are shown. The proposed (SELL) algorithm performs better in terms of detail preserving and contrast preservation. Finer details like eyes, nose, and hair were restored better than all the other algorithms. ACWMMF and DWMF could not restore

TABLE I
SSIM VALUE FOR THE IMAGES OF DIFFERENT SALT AND PEPPER NOISE LEVELS FOR SIX IMAGES

Image/ Noise	House		Boat		Barbara		Baboon		Girl		Airplane	
	DL-INR	SELL	DL-INR	SELL	DL-INR	SELL	DL-INR	SELL	DL-INR	SELL	DL-INR	SELL
10	0.9467	0.9918	0.8552	0.9741	0.9446	0.9912	0.7149	0.9558	0.9661	0.9946	0.8832	0.9830
20	0.9283	0.9779	0.8004	0.9351	0.9241	0.9774	0.6239	0.9060	0.9547	0.9872	0.8641	0.9631
30	0.8947	0.9558	0.7361	0.8884	0.8976	0.9520	0.5136	0.8521	0.9396	0.9726	0.8112	0.9358
40	0.8658	0.9211	0.6406	0.8442	0.8639	0.9099	0.4472	0.7917	0.9229	0.9577	0.7725	0.9002
50	0.8027	0.8915	0.5892	0.7808	0.8162	0.8839	0.3896	0.7184	0.9000	0.9359	0.7212	0.8497
60	0.7501	0.8441	0.5339	0.7285	0.7523	0.8431	0.3494	0.6384	0.8777	0.9212	0.6838	0.8092
70	0.7156	0.8009	0.4869	0.6599	0.7202	0.8030	0.2984	0.5530	0.8620	0.9018	0.6533	0.7582
80	0.7127	0.7708	0.4708	0.6006	0.7131	0.7717	0.2815	0.4595	0.8542	0.8835	0.6356	0.7098

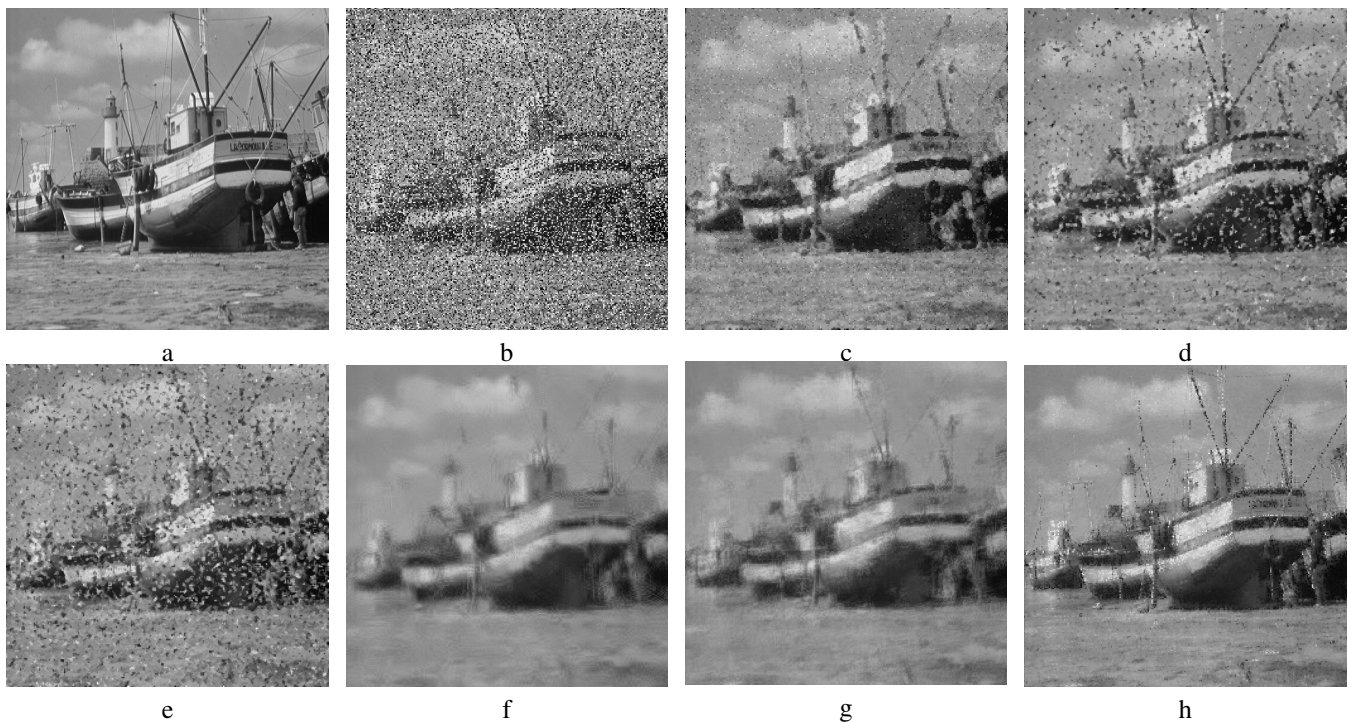


Fig. 11. The denoising results for boat image corrupted by random value impulse noise a) original boat image b) 50% of pixels corrupted by random value impulse noise c) PSMF d) ACWM e) DWM f) $l1l1$ -DCT g) DL-INR h) The proposed method

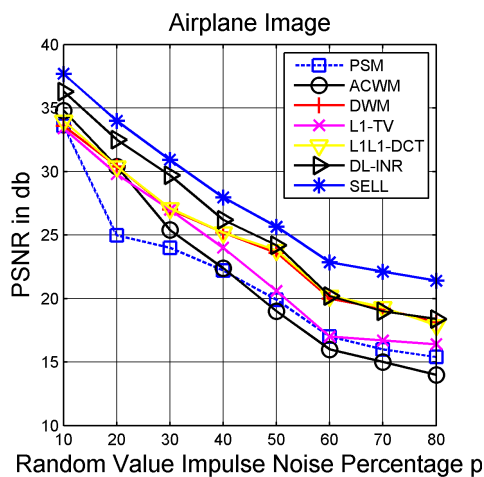


Fig. 12. PSNR values for various percentage of random value impulse noise corrupted pixels in airplane image

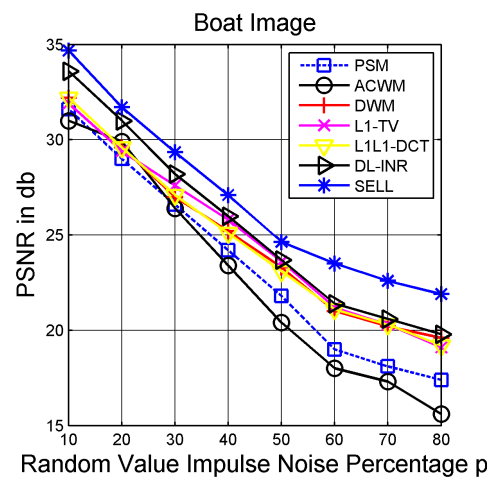


Fig. 13. PSNR values for various percentage of random value impulse noise corrupted pixels in boat image

or recover a any information from the corrupted image as shown in Fig.14 (d) and (e). $l1l1$ -DCT and DL-INR could recover or de-noise the image, but most of the details were blurred. PSNR values were plotted against percentage of

pixels corrupted by the random values impulse noise shown in Fig.15 and PSNR values of the proposed algorithm is higher than other algorithms.

Fig.17 shows the denoising result for house image with

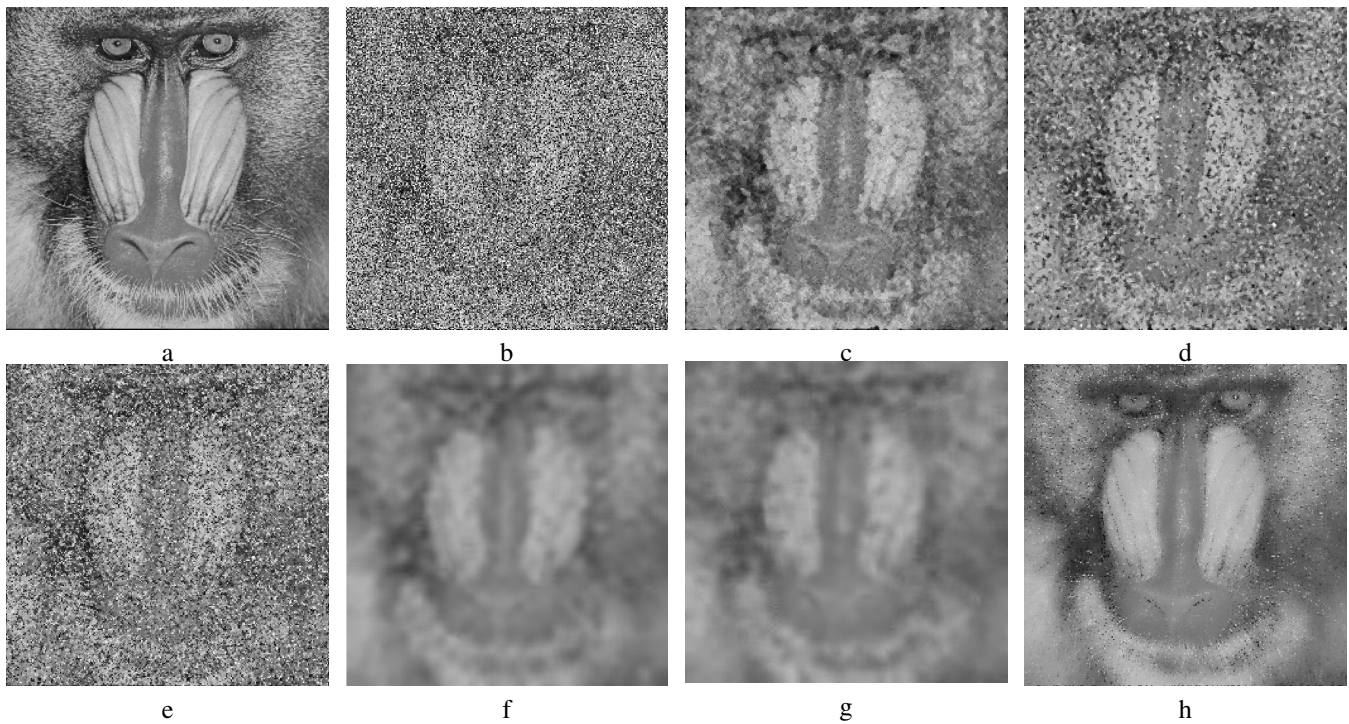


Fig. 14. The denoising results for baboon image corrupted by random value impulse noise a) original baboon image b) 70% of pixels corrupted by random value impulse noise c) PSMF d) ACWM e) DWM f) $\ell_1\ell_1$ -DCT g) DL-INR h) The proposed method

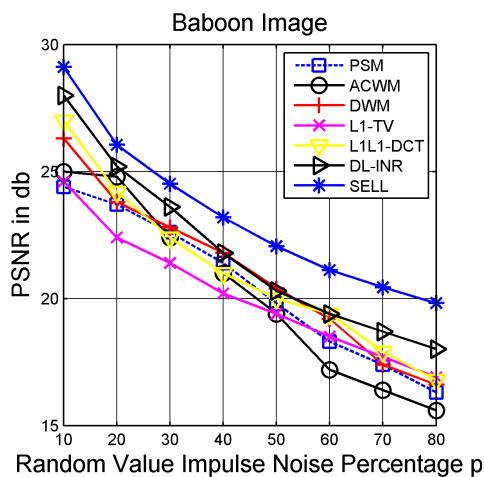


Fig. 15. PSNR values for various percentage of random value impulse noise corrupted pixels in baboon image

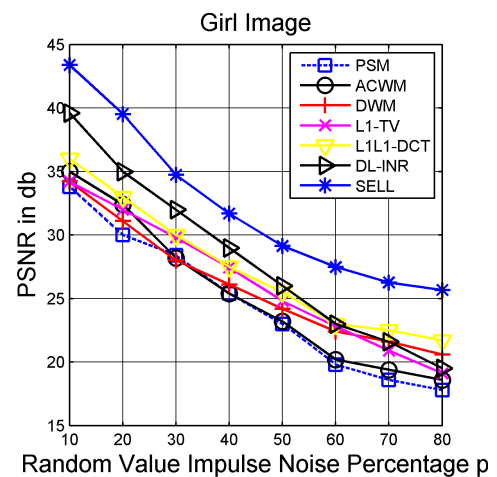


Fig. 16. PSNR values for various percentage of random value impulse noise corrupted pixels in girl image

80% of pixels were corrupted by random value impulse noise. Fig.17 (b) shows the 80% of pixels corrupted image. Fig.17 (c), (d), (e), (f), (g) and (h) shows de-noising result of PSMF, ACWMF, DWMF, $\ell_1\ell_1$ -DCT, DL-INR and the proposed algorithm. spatial domain filters were failed to produce a significant improvement to the corrupted image. The proposed algorithm, DL-INR and $\ell_1\ell_1$ -DCT denoising results were significantly better for 80% of pixels corrupted image. Compared with DL-INR algorithm SELL performs better for high level of noise corrupted images.

Plots between peak signal to noise ratio and 10%-80% percentage of pixels corrupted by random value impulse noise corrupted image shown in Fig.12,13,15,16,18,19. SELL gives consistently better PSNR value than the other algorithms. PSNR improvement in certain test images house and girl are more than 3 db. In higher noise percentage PSNR difference

is much higher than the lower noise percentage, which proves the robustness of the SELL algorithm.

V. DISCUSSIONS

A. Parameter settings

The proposed algorithm has many parameters. Selection of appropriate values for these parameters helps to achieve a better peak signal to noise ratio and visual quality of the image. The parameters were α, β, γ and μ . Among the parameters β directly determines the learning rate of the dictionary. α, γ and μ indirectly influence the learning rate through equation for Lagrangian multiplier λ and sparse coefficient X . β value is fixed at 0.001 for balanced dictionary learning. It has been fixed after heuristics experiments.

Value of α determines the relationship between sparse representation term and data fidelity term. Depending on

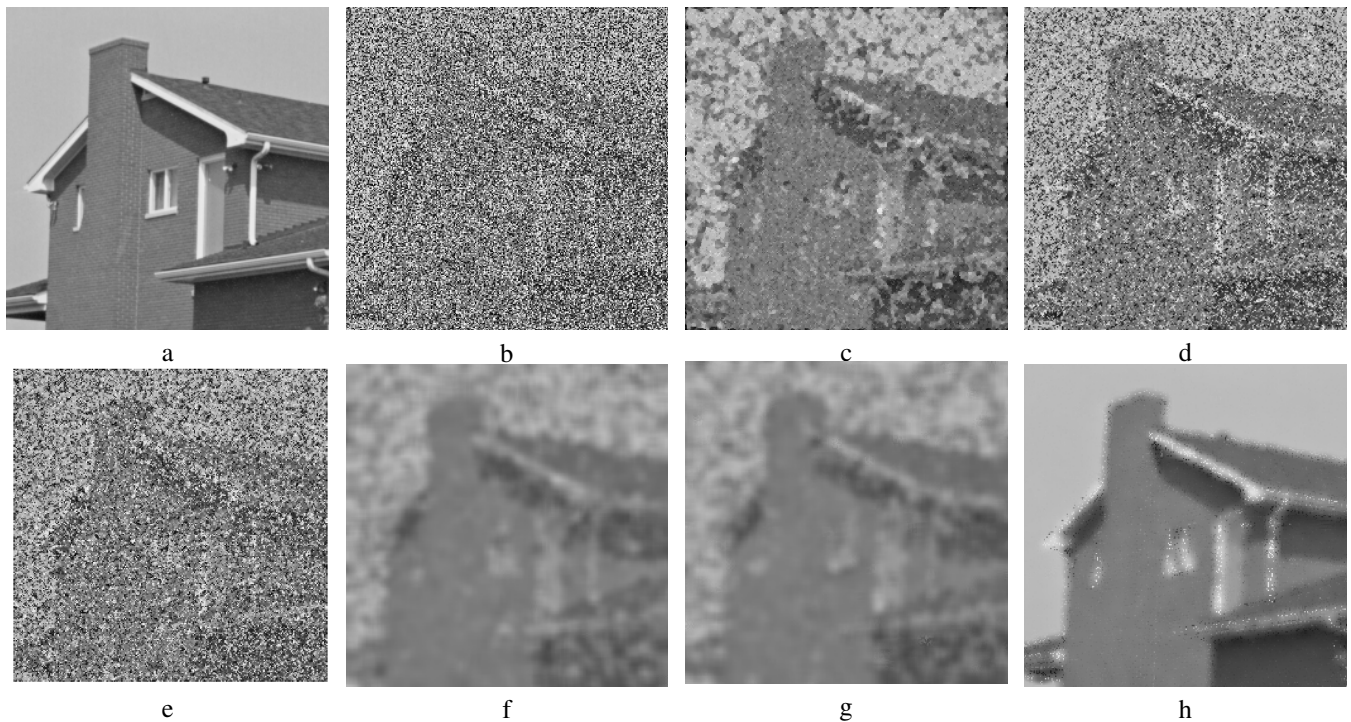


Fig. 17. The denoising results for house image corrupted by random value impulse noise a) original house image b) 80% of pixels corrupted by salt and pepper impulse noise c) PSMF d) ACWM e) DWM f) $\ell_1\ell_1$ -DCT g) DL-INR h) The proposed method

TABLE II
 α VALUES FOR VARIOUS PERCENTAGE OF FIXED VALUE IMPULSE NOISE PIXELS IN DIFFERENT IMAGES

Noise Percentage	10	20	30	40	50	60	70	80
α	0.7295	0.6629	0.5963	0.5375	0.4235	0.3835	0.3235	0.2343

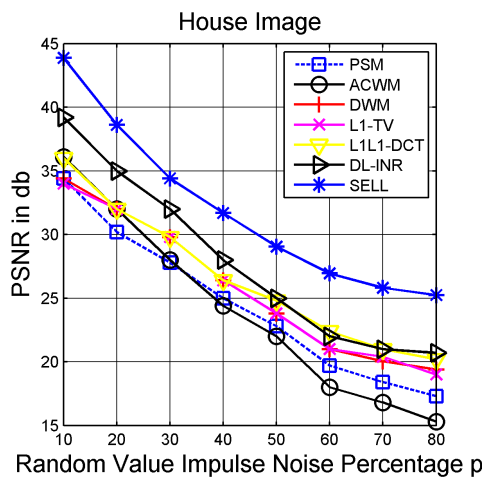


Fig. 18. PSNR values for various percentage of random value impulse noise corrupted pixels in house image

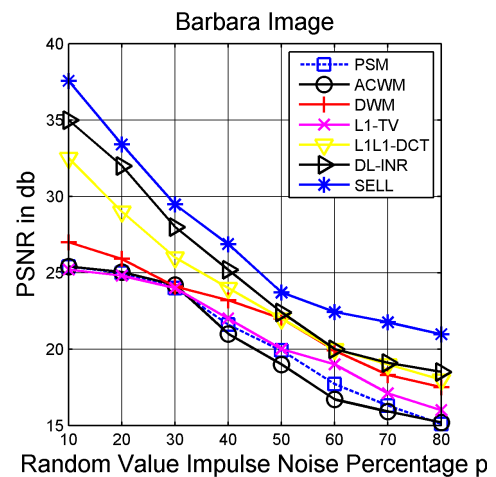


Fig. 19. PSNR values for various percentage of random value impulse noise corrupted pixels in barbara image

α value de-noising performance varies. Highly accurate α value is required for faster learning of dictionary and visual quality. small variation in α value leads to large variation in quality of image and dictionary. Table II gives α value for different noise levels of all images. α is used in Augmented Lagrangian Multiplier equation Y and indirectly influences X and A. For faster convergence, α may be converted to adaptively varying parameter. Further research is required to determine the α values from the corrupted image, instead of tabulation based values.

Another parameter which influences both dictionary (A)

and sparse coefficients (X) is γ whose value is made adaptive by including it in algorithm's steps. γ value is updated by dictionary updates. Initial dictionary values affect γ value. Initial dictionary value may be DCT matrix or random matrix. If random value matrix as a initial dictionary matrix (A), variations in γ value shown in Fig.20, γ value or maximum eigen value decreases from large value to moderate value and stabilizes after 20 iterations. If initial dictionary matrix (A) is DCT matrix, Fig.21 shows that γ value increases from small value and stabilizes after 20 iterations. Our future work will improve the dictionary learning by considering different

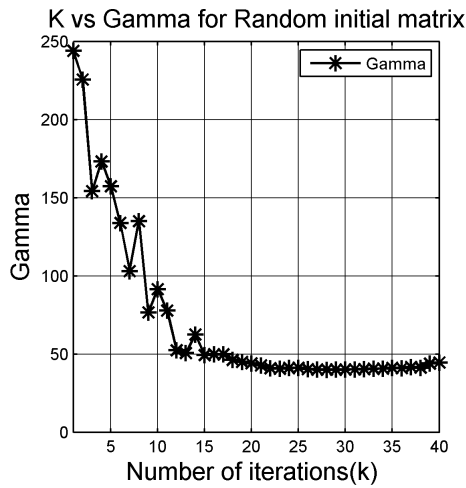


Fig. 20. Maximum eigen value γ for random values as an initial dictionary

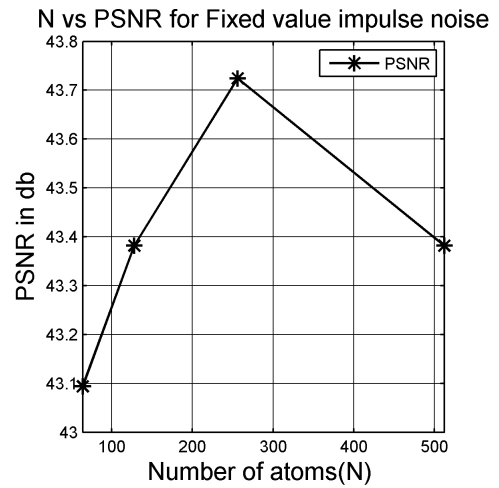


Fig. 23. Number of atoms N in a dictionary and PSNR values

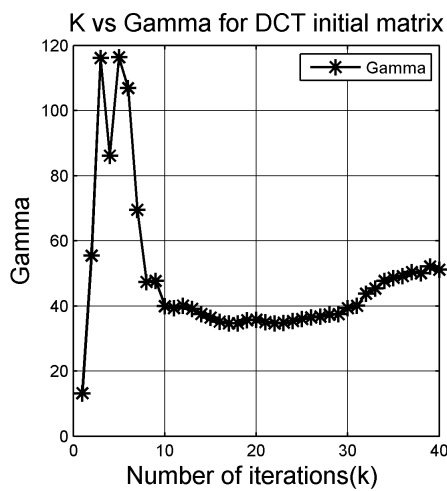


Fig. 21. Maximum eigen value γ for DCT matrix value as an initial dictionary

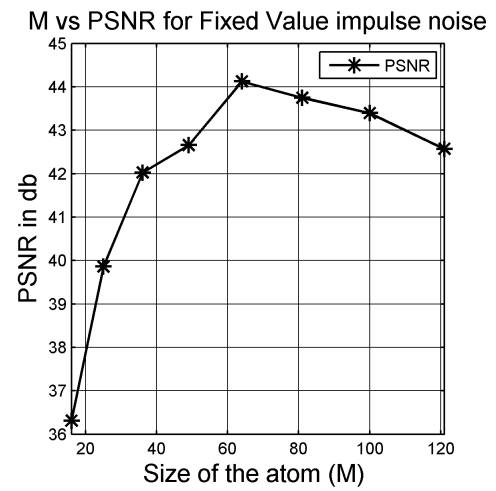


Fig. 24. Number of elements in an atom M and PSNR value

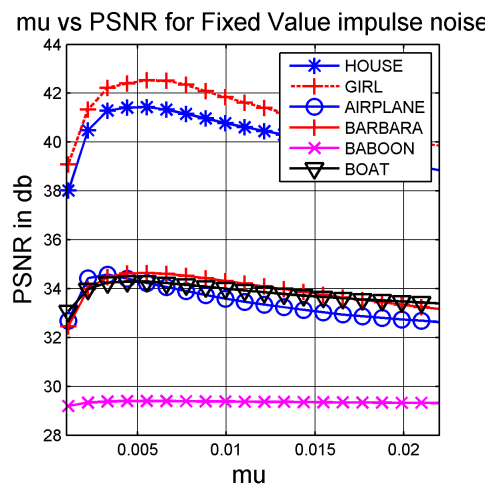


Fig. 22. various μ values and PSNR value

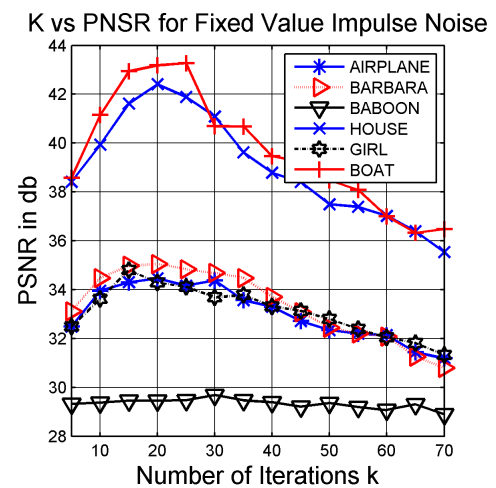


Fig. 25. Number of Iterations K for algorithm and PSNR value

initial values like walsh, hadamard, haar transform matrices as a initial dictionary.

From Fig.22 μ value is fixed at 0.006 after calculating PSNR values for the range of 0.001 to 0.009. For $\mu=0.006$ value all standard images used in this algorithm attains maximum PSNR value. Dictionary size is also important for

better PSNR and SSIM [20] values. For K-SVD [29], DL-INR [9], ALM [11] algorithms dictionary size is 64×256 . Dictionary size for this algorithm is obtained by plotting PSNR value against number of atoms in a dictionary (N). N value varied from 81 to 512. For 256 atoms in a dictionary PSNR reaches the maximum value as shown in Fig.23 and N is fixed at 256.

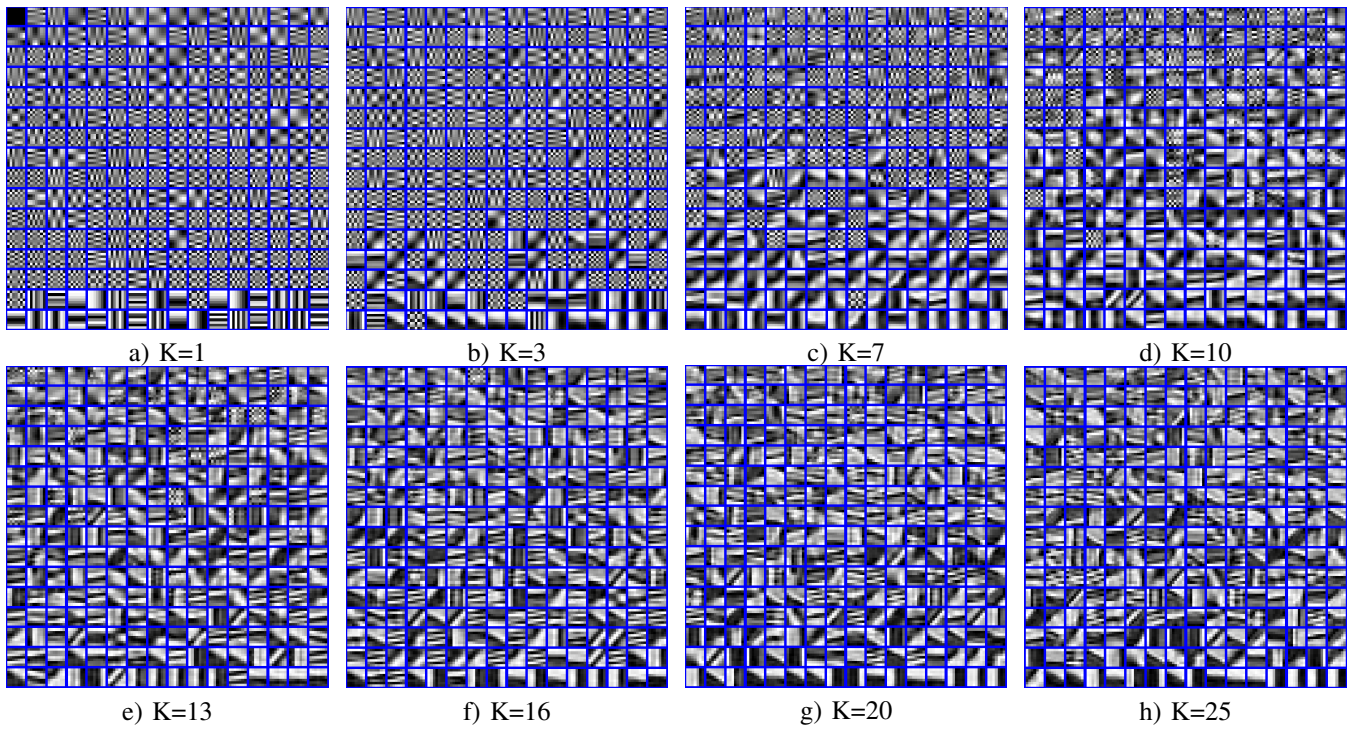


Fig. 26. Learned dictionary for different iterations of the algorithm for 10% random value impulse noise corrupted house image and DCT matrix as a initial value

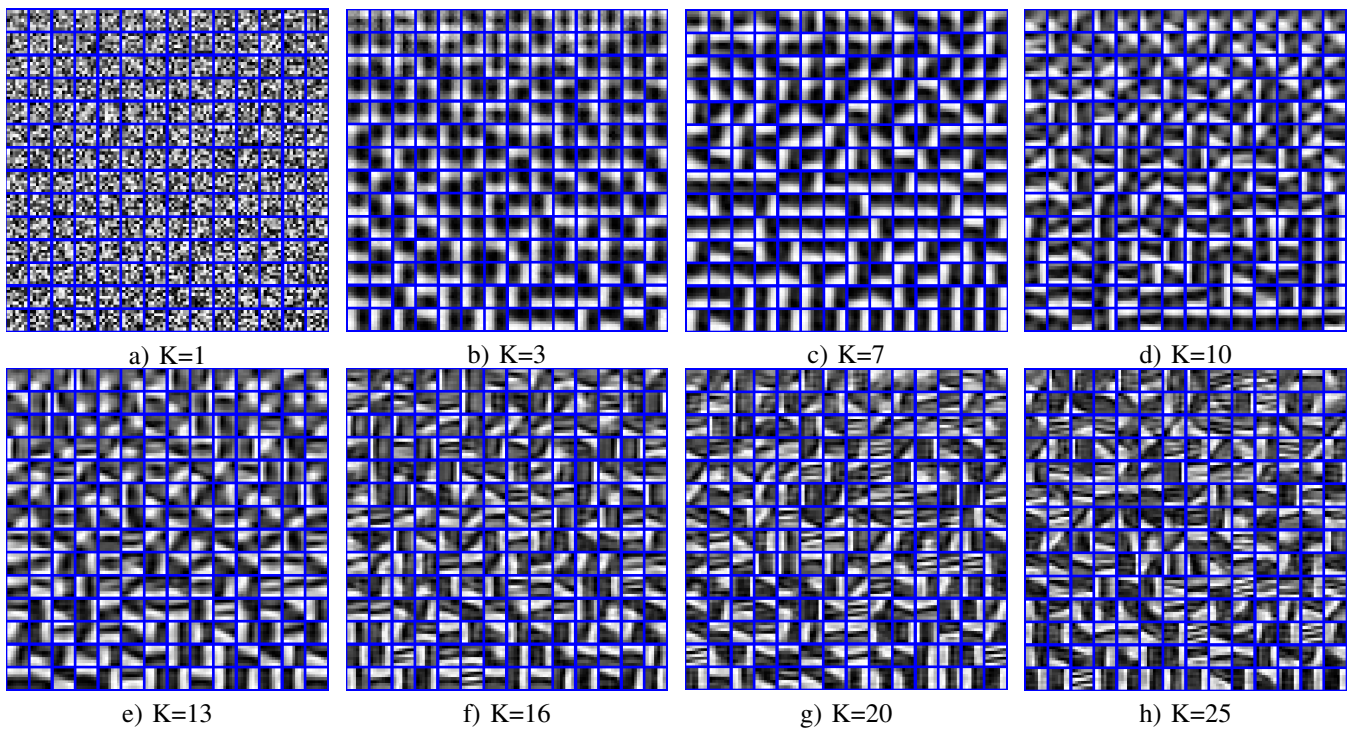


Fig. 27. Dictionary for different iterations of the algorithm for 10% random value impulse noise corrupted house image and random value as a initial Dictionary value

In order to determine the number elements in an atom (M), PSNR value is plotted against M value. Fig.24 shows the plot for PSNR and M value, M value ranges from 16 to 121. PSNR peaks at M=64. From the above conclusion dictionary size for this algorithm is 64×256 .

Number of iterations required for this algorithm is determined after calculating PSNR value for various number of iterations(K), which is shown in Fig.25. For K value 25 this algorithm attains maximum PSNR value. The number

of iterations is fixed at 25 for all images and both fixed value and random value impulse noises. From number of experiments conducted for different test images, number of non-zero elements in the sparse coefficient matrix X decreases with increase in noise density for both salt and pepper impulse noise and random value impulse noise. It is observed that the number of non-zero elements in X is very sparse for 80% noise level.

Fig.26 shows the dictionary learned during many iterations

TABLE III
AVERAGE EXECUTION TIME FOR DIFFERENT IMAGES AND NOISE PIXEL PERCENTAGES (TIME IN SECONDS)

algorithm/ Noise%	10	20	30	40	50	60
PSMF	1	1	1	1	1	1
ACWM	56	57	57	56	56	56
DWM	258	257	257	257	256	256
L1-TV	10	13	14	14	16	17
$\ell_1\ell_1$ -DCT	74	74	72	70	67	65
AK-SPR	2153	1581	1567	904	1101	1815
DL-INR	81	81	79	77	74	72
SMLL	51	52	52	52	52	52

of algorithm with DCT matrix as an initial dictionary matrix. Fig.27 shows the dictionary learned during many iterations of algorithm with random matrix as a initial dictionary matrix. From Fig.26,27 final dictionary appears to be similar for different initial values for dictionary and proves the robustness of the algorithm for different initial values of dictionary.

B. Computational analysis

Our algorithm was implemented in MATLAB2007 with computer containing an Intel Core2 Duo T7500 processor at 2.00GHz speed and 2GB DDR RAM. Computational time was greatly reduced by converting a two stage algorithm in $\ell_1-\ell_1$ minimization into single stage algorithm. By choosing appropriate values for parameters, the number of iterations was reduced. And combining the similar terms in the algorithms, redundant computations were removed, which in turn reduced computation required for efficient calculations of X and A. Average time was calculated for six images of 10 experiments per noise level, for both impulse and random value noise being tested and tabulated in Table III. Image size was restricted to uniform 256 x 256. The proposed SELL algorithm is faster than the DL-INR algorithm, AK-SPR, and $\ell_1\ell_1$ -DCT algorithm. In $\ell_1\ell_1$ -DCT dictionary is not updated as in DL-INR, SELL algorithms, so it is faster than DL-INR but slower than SELL. The proposed SELL is faster due to optimization and simplification of algorithm steps to reduce the number of multiplications and additions and modification in implementation of PROJ and SHRINK.

VI. CONCLUSION

In this paper spatial and efficient $\ell_1-\ell_1$ minimization based fixed and random valued impulse noise removal algorithm was presented. Image batches formed from noisy image. In noisy image, noisy pixels were identified using any impulse noise detector and from noise free pixels DC values were calculated. DC values were subtracted from noisy image batches. Before applying denoising algorithms on noisy image, similar pixel batches were grouped. From each group representation batches were used for denoising. The $\ell_1-\ell_1$ minimization algorithm was modified into single stage algorithm from two stage algorithm in order to reduce the number of iterations required for de-noising and reducing the computation time. After denoising representative batches were used to replace all similar noisy batches. Accurate DC value calculation improved the edge preservation and noise suppression. Our algorithm results were compared

with spatial domain methods and sparse representation based algorithms. The proposed algorithm outperforms all other algorithms in terms of de-noising performance and preserving image details. In our future work we intend to apply our algorithm to color images, artifacts removal and also to improve the updation speed of the ALM coefficients and modify the algorithm for very high density noise images.

REFERENCES

- [1] J.Astola, P.Kuosmanen, *Fundamentals of Nonlinear Digital Filtering*, CRC Press, Newyork, 1997.
- [2] I.Pitas, A.N.Venetsanopoulos, *Non linear Digital Filters, Principles and Applications*, Springer Science, 1990.
- [3] David.C.Lay, *Linear Algebra and Its Applications*, Addison-Wesley, Reading, MA, 1994.
- [4] Z. Wang and D. Zhang, "Progressive switching median filter for the removal of impulse noise from highly corrupted images", *IEEE Transactions on Circuits and Systems*, vol.46, pp.78-80, 1999.
- [5] T. Chen and H. R. Wu, "Adaptive impulse detection using Center-Weighted median filters", *IEEE Signal processing letters*, vol.8, pp.1-3, Jan 2001.
- [6] Y. Dong and S. Xu, "A new directional weighted median filter for removal of random-valued impulse noise", *IEEE Signal Processing Letters*, vol.14, no.3, pp.193-196, 2007.
- [7] M. Nikolova, "A variational approach to remove outliers and impulse noise", *Journal of Mathematical Imaging and Vision*, vol.20, no. 1-2, pp.99-120, 2004.
- [8] P. Bouboulis, K. Slavakis and S. Theodoridis, "Adaptive kernel-based image denoising employing semi-parametric regularization", *IEEE Transactions on Image Processing*, vol.19, no.6, pp.1465-1479, 2010.
- [9] S. Wang, Q. Liu, Y. Xia, P. Dong, J. Luo, Q. Huang and D. D. Feng, "Dictionary learning based impulse noise removal via $\ell_1-\ell_1$ minimization", *Signal Processing*, vol.93, no.9, pp.2696-2708, 2013.
- [10] Q. Liu, J. Luo, S. Wang, M. Xiao and M. Ye, "An augmented Lagrangian multi-scale dictionary learning algorithm", *EURASIP Journal on Advances in Signal Processing*, vol.2011, no.1, pp.1-16, 2011.
- [11] Q. Liu, S. Wang, J. Luo, Y. Zhu and M. Ye, "An augmented Lagrangian approach to general dictionary learning for image denoising", *Journal of Visual Communication and Image Representation*, vol.23, no.5, pp.753-766, 2012.
- [12] S.H.Chan, R.Khoshabeh, K.B.Gibson, P.E.Gill, T.Q.Nguyen, "An Augmented Lagrangian Method for Total Variation Video Restoration", *IEEE Transactions On Image Processing*, vol.20, pp.3097-3111, 2011.
- [13] D. L. Donoho, "Compressed sensing", *IEEE Transactions on Information Theory*, vol.52, no.4, pp.1289-1306, 2006.
- [14] D. P. Bertsekas, *Constrained Optimization and Lagrange Multiplier Method's*, Athena Scientific, Reimont, MA, 1982.
- [15] M. Elad and M. Aharon, "Image denoising via sparse and redundant representations over learned dictionaries", *IEEE Transactions on Image Processing*, vol.15, no.12, pp.3736-3745, 2006.
- [16] M. Aharon, M. Elad and A. M. Bruckstein, "On the uniqueness of overcomplete dictionaries, and a practical way to retrieve them", *Linear Algebra and Applications*, vol.416, pp.48-67, 2006.
- [17] M. Elad, *Sparse and redundant representations from theory to applications in signal and image processing*, Springer, 2010.
- [18] S.J.Horng, L.Y. Hsu, T.Li, S.Qiao, X.Gong, H.H.Chou, M.K.Khan, "Using Sorted Switching Median Filter to remove high-density impulse noises", *Journal of Visual Communication and Image Representation*, Volume 24, Issue.7, pp.956-967, October 2013.
- [19] Isabel M.P.Duarte, Jose M.N.Vieira, Paulo.J.S.G. Ferreira and Daniel F.Albuquerque, "High resolution spectral Estimation Using BP via Compressive sensing", in *Lecture Notes in Engineering and Computer Science: Proceedings of The World Congress on Engineering and Computer Science 2012, WCECS 2012*, 24-26 October, 2012, San Francisco, USA, pp.699-704.
- [20] Z. Wang, A. C. Bovik, H. R. Sheikh, and E. P. Simoncelli, "Image quality assessment: From error measurement to structural similarity", in *IEEE Transactions on Image Processing*, vol.13, no.4, pp.600-612, 2004.
- [21] Subramanyam Ravishankar, Nagadastagiri Reddy, C and M.V.Joshi, "Single Image Super Resolution Using Sparse Image and GLCM statistics as priors", *Lecture Notes in Engineering and Computer Science: Proceedings of The World Congress on Engineering 2011, WCE 2011*, 6-8 July, 2011, London, U.K., pp.1563-1566.
- [22] Allen Y. Yang, Zihan Zhou, Arvind Ganesh, S. Shankar Sastry, Yi Ma, "Fast ℓ_1 -Minimization Algorithms For Robust Face Recognition", *IEEE Transactions on Image Processing*, vol.22, no.8, pp.3234-3246, 2013.

- [23] M.Andrecut, "Sparse Random Approximation and Lossy Compression", *IAENG International Journal of Applied Mathematics*, vol.38, no.3, pp205-214, 2004.
- [24] A.Gramfort, C.Poupon, M.Descoteaux, "Denoising and fast diffusion imaging with physically constrained sparse dictionary learning".*Medical Image Analysis*, Vol.18, pp.36-49, 2014.
- [25] M.R. Mohammadi, E. Fatemizadeh, M.H. Mahoor, "PCA based dictionary building for accurate facial expression recognition via sparse representation", *Journal of Visual Communication and Image Representation*, vol.25, pp.1082-1092, 2014.
- [26] M.Zhao, S.Li, J.Kwok, "Text detection in images using sparse representation with discriminative dictionaries", *Image and Vision Computing*, vol.28, pp.1590-1599, 2010.
- [27] Ran Xu, Jianbin Jiao, Baochang Zhang, Qixiang Ye, "Pedestrian detection in images via cascaded ℓ_1 norm minimization learning method", *Pattern recognition*, vol.45, pp.2573-2583, 2012.
- [28] Y.Xiao, T.Y.Zeng, J.Yu, M.K.and Ng, "Restoration of images corrupted by mixed Gaussian-impulse noise via ℓ_1 - ℓ_0 minimization", *Pattern recognition*, vol.44, pp.1708-1720, 2011.
- [29] Michal Aharon, Michael Elad, and Alfred Bruckstein, "K-SVD: An Algorithm for Designing Overcomplete Dictionaries for Sparse Representation", *IEEE Transactions on Signal Processing*, vol.54, pp.4311-4322, 2006.
- [30] Rauhut, H., Schnass, K., and Vandergheynst, P., "Compressed Sensing and Redundant Dictionaries", *IEEE Transactions on Information Theory*, vol.54, pp.2210-2219, 2008.
- [31] Gribonval, R., Schnass, K., "Dictionary identification: sparse matrix-factorization via ℓ_1 -minimization", *IEEE Transactions on Information Theory*, vol.56, pp.3523-3539, 2010.
- [32] W.Yin, S.Osher, D.Goldfarb, J.Darbon, "Bregman iterative algorithms for ℓ_1 minimization with application to compressed sensing", *SIAM Journal on Imaging Sciences*, vol.1, no.1, pp.143-168, 2008.



P.Jothibasu was born in 1978 in India. He received B. E. from Bharathiyar University and M. E. from Anna university. Presently he is doing part time doctoral degree in Anna University, Chennai. Currently he is working as an Assistant Professor in Electronics and Instrumentation Engineering Department, R.M.K Engineering College, Chennai. His research interests are signal processing, Image processing and embedded systems.



P.Rangarajan was born in 1969 in India. He received B. E. in Electrical and Electronics Engineering from Bharthiyar University, M.E. and Ph. D. from Anna University. He is presently working as a Professor in Electrical and Electronics Engineering Department, R.M.D. Engineering College, Kavaraipettai, Chennai. His research interests are VLSI, VLSI system Design, signal processing and Image processing. He has successfully guided many doctoral degree scholars. He also carried out research projects funded by national and international Organizations.

tional Organizations.